

Nonlinear magnetotransport and charge-density-wave motion in NbSe₃ at temperatures from 1.2 to 50 K

R. V. Coleman, M. P. Everson, G. Eiserman, and A. Johnson
Physics Department, University of Virginia, Charlottesville, Virginia 22901
 (Received 20 December 1984)

The transverse magnetoresistance of NbSe₃ at 1.2 K shows a large non-Ohmic reduction as a function of electric field for magnetic fields in the range 50–230 kG. The magnetoresistance data in the temperature range 1.2–43 K have been fitted to a Zener-tunneling model of the form $\sigma = \sigma_a(H) + \sigma_b(1 - E_T/E) \times \exp(-E_0/E)$ and give a value of $E_0 = 0.47$ V/cm and $E_T = 0.066$ V/cm at 1.2 K and 206 kG for a crystal with a residual resistance ratio of 145. At 206 kG E_0 follows a temperature dependence of the form $E_0(T) = E_0(0) \exp(-k_B T/\Delta)$ with $\Delta/k_B = 15.2$ K. The threshold electric field for charge-density-wave (CDW) motion is reduced at high magnetic fields and low temperatures while the magnetoresistance behavior suggests that the CDW structure below 59 K is strongly coupled to the magnetic field.

We report on measurements of the transverse magnetoresistance in NbSe₃ at a temperature of 1.2 K in a magnetic field range 0–230 kG and make comparisons to magnetoresistance measurements at higher temperatures. Two charge-density waves^{1,2} (CDW's) form in NbSe₃ with transition temperatures of 144 and 59 K. At $H=0$ the conductivity below these transitions shows a nonlinear increase above certain threshold electric fields^{3,4} due to the onset of sliding motion⁵ of the CDW; however, at $H=0$ these threshold electric fields become large at very low temperatures.⁴ We conclude that the threshold electric field E_T is lowered by the magnetic field and that CDW motion can take place at very low temperatures and high magnetic fields.

At 1.2 K a reduction of the transverse magnetoresistance as a function of electric field is observed which is very similar to that previously reported^{6,7} at 20 and 30 K. The data over the entire temperature range can be fit quite well to the functional form introduced by Bardeen⁸ for electric-field-induced tunneling of the CDW,

$$\sigma = \sigma_a(H) + \sigma_b(1 - E_T/E) \exp(-E_0/E),$$

where $\sigma_a(H)$ is the magnetoconductivity and σ_b is a magnetic-field-independent conductivity due to the tunneling channel. E_T is the threshold electric field required for CDW motion and E_0 is related to the pinning gap. The non-Ohmic magnetoresistance is observable above ten kilogauss for sufficiently high electric fields and the tunneling gap is of the same order as found for CDW motion, while the threshold electric fields required for tunneling at high magnetic fields and low temperature are greatly reduced from the values expected at $H=0$.

The crystals grow in a monoclinic crystal structure with the axis of the crystal along the **b** axis. The transverse magnetoresistance data have been measured with $I \parallel \mathbf{b}$ and $H \parallel \mathbf{c}$ although similar effects are observed for other orientations of H . The crystals have residual resistance ratios (RRR) in the range 60–160 and no major differences in the magnetic-field effects have been observed except for the expected changes in E_0 and E_T as a function of impurity content.⁹

The data shown here were recorded from a crystal with a RRR of 145. Figure 1 shows the measured voltage along the crystal for measuring currents in the range 2–100 mA as

the magnetic field is swept from 0 to 230 kG at a temperature of 1.2 K. At less than 10 kG, the resistance is approximately Ohmic for the current range 2–100 mA, while at 10 kG and above, the resistance becomes progressively more non-Ohmic as the magnetoresistance term becomes larger. At 230 kG, the resistance decreases by a factor of 4 as the current is increased from 2 to 100 mA. This non-Ohmic behavior is immediately evident from the direct data of Fig. 1 since, above 50 kG, the slope of the curve and the amplitude of the oscillations show only a very slow increase as the current is increased from 20 to 100 mA.

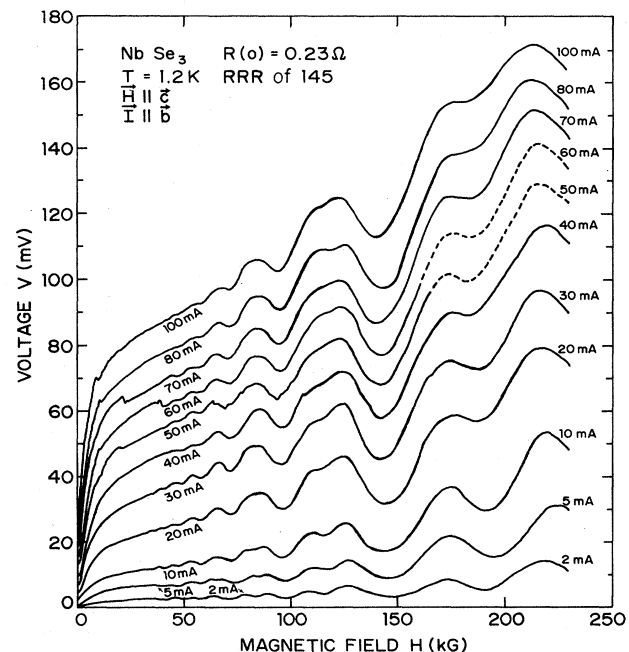


FIG. 1. Voltage drop measured along the crystal as a function of transverse magnetic field in the range 0–230 kG at 1.2 K. Curves are shown for measuring currents of 2–100 mA. At magnetic fields below ~ 10 kG the voltage increase with current is nearly Ohmic while at high magnetic fields the voltage increase with current is much less than required for Ohmic behavior.

If the data in Fig. 1 are replotted as I vs V curves at constant magnetic field then above 10 kG the resistance becomes nonlinear at progressively lower currents as the magnetic field is increased. The same data can be generated by holding the magnetic field constant and varying the current in the range 2–100 mA. In both cases the magnetic resistance at 1.2 K shows a decrease characteristic of CDW motion above a critical threshold electric field.

The magnetic resistance transition is not sharp and occurs continuously from low currents up to current values where the magnetic resistance approaches saturation. The continuous magnetic resistance transition is demonstrated in Fig. 2(a), where the magnetic resistance at 230 kG and 1.2 K is plotted as a function of longitudinal electric field. Data obtained from the same crystal in 206 kG at 20 and 30 K are also plotted in Fig. 2(a). The ratio $R(E)/R(0)$ has been plotted where $R(0)$ is the magnetic resistance value deter-

mined for the lowest measuring current. In all cases, the reduction starts at low electric fields and approaches saturation at progressively higher electric fields as the temperature is lowered. The solid curves represent fits to the functional dependence expected for the Zener tunneling model.

The non-Ohmic reduction of magnetoresistance could be interpreted as due either to the opening of a new current channel which does not contribute to the magnetoresistance, or to a similar electric-field-induced electron-tunneling process, which modifies a direct contribution of the CDW to the magnetoresistance of the normal electrons. In either case, a similar functional dependence of the tunneling probability on electric field at constant magnetic field and temperature would result. In the case of CDW motion at $H=0$, Bardeen's^{8,10} proposed Zener tunneling model gives $I_{CDW} = G_b(E - E_T)e^{-E_0/E}$, where G_b is the CDW conductance, E_T is the threshold electric field required for CDW motion, and E_0 is a constant related to the pinning gap.

The magnetic resistance data above 200 kG at 1.2, 20, and 30 K have been fit to the Zener tunneling model using the following expression for the relative resistance change as a function of longitudinal electric field:

$$\frac{R(E)}{R(0)} = \left[1 + \frac{\sigma_b}{\sigma_a(H)} \left(1 - \frac{E_T}{E} \right) e^{-E_0/E} \right]^{-1}, \quad (1)$$

where $\sigma_b/\sigma_a(H)$ is the ratio of the CDW associated conductivity to the magnetoconductivity observed at low electric field. The best fits to the present data are obtained with very small or zero values of E_T . The solid curves shown in Fig. 2(a) are obtained with small values of E_T as listed in the figure. This is consistent with the bell shape of the magnetic-resistance curves, which do not exhibit the sharp onset expected for large electric field thresholds. Three parameter fits obtained by requiring the largest values of E_T consistent with the data at the higher electric fields are shown in Fig. 2(b). It is clear that the three parameter fits with small E_T values as shown in Fig. 2(a) give better fits to the data at low electric fields. Even the largest values of E_T used in Fig. 2(b) are still significantly lower than those measured at $H=0$. For example, at 20 K, $E_T \geq 0.1$ V/cm at $H=0$, while at $H=206$ kG the fit in Fig. 2(b) gives $E_T(\text{max}) = 0.035$ V/cm. At much higher temperatures, where E_T is already small at $H=0$, the magnetic field does not produce a strong modification of E_T as demonstrated in Fig. 3 for data recorded at 43 K. Using the value of $E_T = 0.013$ V/cm measured at 43 K and 206 kG and assuming the same temperature dependence of E_T as derived for E_0 below, we are able to generate a good fit to all of the data using the values of E_0 and E_T as listed in Fig. 2(a).

The temperature dependence of E_0 follows the functional form $E_0(T) = E_0(0) \exp(-k_B T/\Delta)$ as shown in Fig. 4 with $E_0(0) = 0.50$ V/cm and $\Delta/k_B = 15.2$ K. If this is interpreted as a fluctuation term, then Δ is an energy on the order of 10^{-15} ergs (~ 1 meV). The same temperature dependence has been used to generate values of E_T at low temperatures and high magnetic fields, as also shown in Fig. 4. The measured value of $E_T = 0.013$ V/cm at 43 K and 206 kG has been used giving a value of $E_T(0) = 0.070$ V/cm at $T=0$. This analysis implies that the ratio E_0/E_T is a constant independent of temperature and equal to ~ 7.0 . The values of E_0 derived from the above fits are in close agreement with those measured by Brill and co-workers⁹ at $H=0$ for a NbSe₃ crystal with an RRR of 173. They obtained

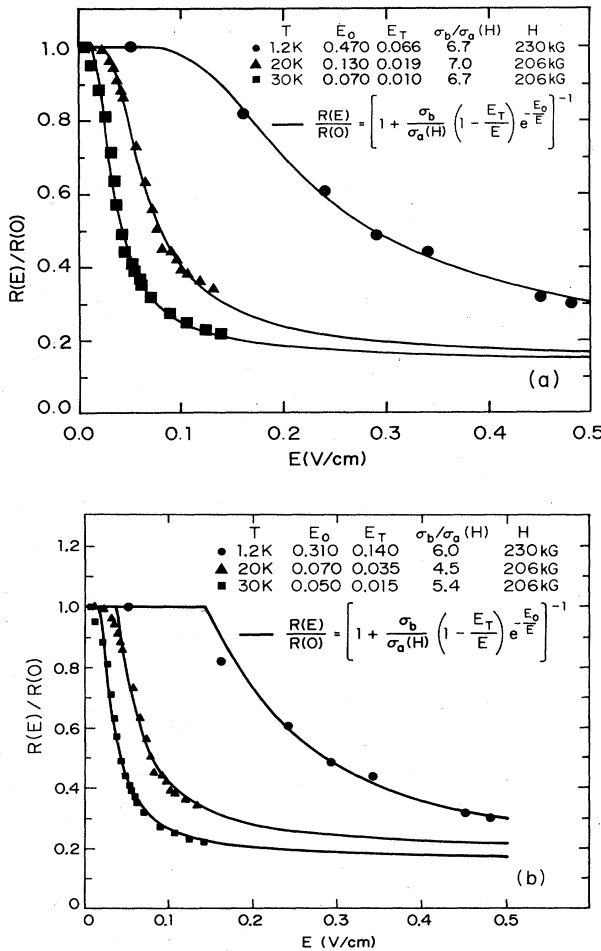


FIG. 2. Magnetic resistance at electric field E divided by magnetic resistance at $E \approx 0$ vs applied electric field. (a) Data above 200 kG at 1.2, 20, and 30 K. The solid curves are fits to Eq. (1) with values of E_T generated from the temperature dependence shown in Fig. 4 and consistent with a substantial reduction from the values measured at $H=0$. (b) Fits to the same data as in (a) above, but using the largest values of E_T allowed by the data points at high electric fields. Values of E_0 , E_T , and $\sigma_b/\sigma_a(H)$ are listed in each figure.

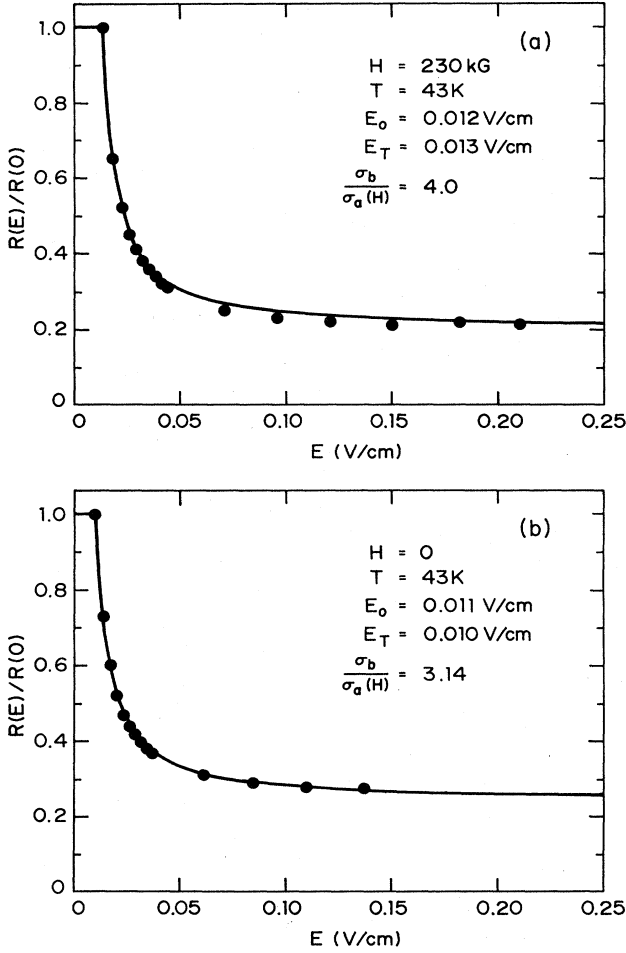


FIG. 3. Magnetic resistance at electric field E divided by the magnetic resistance at $E \approx 0$ vs applied electric field at 43 K. Solid curves are fits to Eq. (1) with computer-generated values of the parameters E_0 , E_T , and $\sigma_b/\sigma_a(H)$, as listed in each figure. (a) $H = 230$ kG. (b) $H = 0$ kG.

$E_0(20 \text{ K}) = 0.125$ V/cm and $E_0(30 \text{ K}) = 0.075$ V/cm, while their values of E_T were $E_T(20 \text{ K}) = 0.050$ V/cm and $E_T(30 \text{ K}) = 0.040$ V/cm, significantly higher than the values required to fit the present data at $H = 206$ kG [see Fig. 2(a) for comparisons].

With $E_0(0) = 0.50$ V/cm the electric field breakdown gap can be estimated from $E_0 = \pi E_g^2 / 4 h e^* v_F$. With $e^* = e$ and the Fermi velocity $v_F \approx 10^8$ cm/sec, this gives $E_g \approx 10^{-17}$ ergs. With Bardeen's proposed expression $e^* = em^* / (m^* + M_F)$, where m^* is the band mass and M_F is the Fröhlich mass associated with ion motion, the gap would be much smaller and, in either case, E_g is much smaller than $k_B T$. In Bardeen's theory^{8,10} of CDW depinning this problem is resolved by considering the transmission of the entire CDW. This would involve energies much larger than $k_B T$ since E_g must be multiplied by a large factor in considering CDW tunneling rather than electron tunneling.

The above data suggest the need to consider several possibilities. The magnetic field can cause a change in the Fermi surface and a change in the ratio of normal to condensate electrons. Magnetic-field-induced fluctuations of the

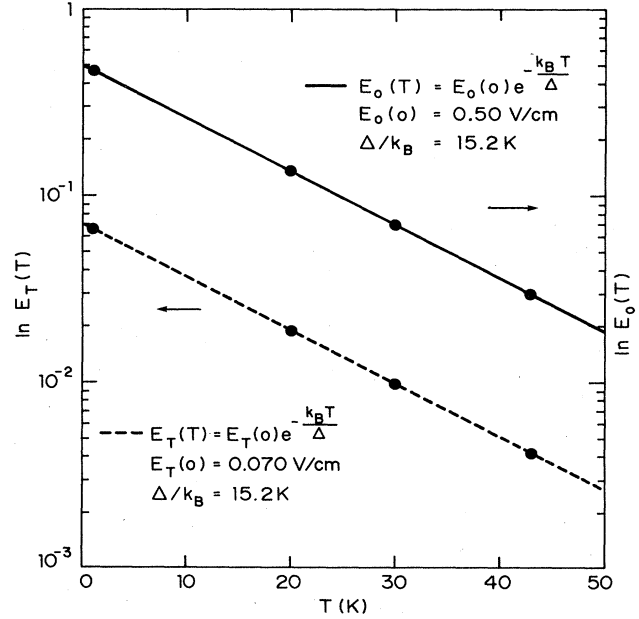


FIG. 4. Temperature dependence of E_0 and E_T at 206 kG in the range 1.2–43 K. The solid straight line follows the functional dependence $E_0(T) = E_0(0) \exp(-k_B T / \Delta)$, where $E_0(0) = 0.50$ V/cm and $\Delta/k_B = 15.2$ K. The dashed straight line follows the functional dependence $E_T(T) = E_T(0) \exp(-k_B T / \Delta)$ with $E_T(0) = 0.066$ V/cm and $\Delta/k_B = 15.2$ K. The value of E_T at 43 K has been taken from the data of Fig. 3(a).

CDW or a change in the Fermi-surface gap structure could lower the threshold electric fields required for CDW motion at low temperature. In either case, motion of the CDW nearly quenches the magnetoresistance in the same way as the resistance anomaly at $H = 0$ is quenched, and therefore suggests an enhanced current flow associated with the CDW motion in a magnetic field.

In order to examine the CDW motion problem in further detail, selected data from these experiments have been replotted in Fig. 5, which shows the resistance at 206 kG as a function of temperature at constant electric fields of $E = 5, 25, 64, 80,$ and 150 mV/cm. At $H = 206$ kG and $E = 5$ mV/cm, little or no resistance depression is observed over the entire temperature range. The resistance as a function of temperature at $H = 0$ and $E = 1$ mV/cm (where no CDW motion takes place) is shown for comparison. Comparing the two curves at 206 and 0 kG calls attention to the point that the magnitude of the magnetic-field-induced resistance increases at intermediate temperatures and reaches a maximum at ~ 30 K. The two curves at $H = 206$ kG and $H = 0$ show a systematic shift at all temperatures indicating an enhanced magnetic resistance not exhibiting the usual $\omega_c \tau$ dependence expected for the normal electron conduction system.

The systematic decrease of the magnetic resistance as a function of electric field at 206 kG is evident. The maxima occurring at 30 K indicate the conditions under which the magnetic increase in resistance becomes overbalanced by the increased CDW tunneling at higher temperatures for a given electric field and the accompanying decrease in resistance. At 30 and 43 K for $E \geq 100$ mV/cm the magnetic-

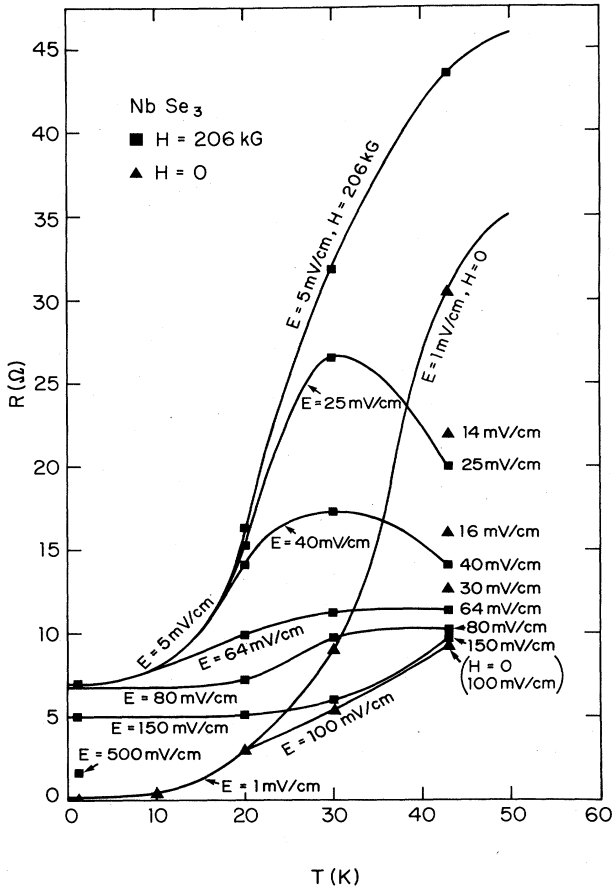


FIG. 5. Temperature dependence of the resistance at 206 kG at constant electric fields of 5, 25, 40, 64, 80, and 150 mV/cm. (■) The temperature dependence of resistance at $H=0$ and $E=1$ mV/cm is also shown. (▲) At the lowest electric fields the magnitude of the magnetoresistance can be seen by comparing the $H=206$ kG and $H=0$ curves represented by the two main parallel curves. At higher electric fields, the resistance curves at 206 kG develop maxima at 30 K which decrease until at $E=150$ mV/cm the resistance shows a monotonic increase with temperature reaching values at 30 and 43 K nearly equal to the resistance at $E > 100$ mV/cm and $H=0$.

field-induced resistance has been nearly quenched and the resistance at 206 kG has decreased to values nearly equal to those observed at $H=0$ and $E=100$ mV/cm. This suggests that both the magnetoconductivity and the conductivity in high electric fields above threshold are effectively determined by CDW motion which quenches the CDW structure contribution to both the resistance and magnetoresistance.

Below 25 K the magnetic resistance at $E=150$ mV/cm crosses over the $H=0$ resistance curve since at lower temperatures electric fields greater than 150 mV/cm are required to obtain further reduction of the magnetic resistance. So far this has only been achieved at 1.2 K, where electric fields up to 500 mV/cm at 206 kG can be applied before reaching the effective power-dissipation limit due to contact heating. At $E=500$ mV/cm and 1.2 K the magnetic resistance is reduced by an additional 60%, as indicated in Fig. 5.

The data as analyzed above indicate a strong coupling of the magnetic field to the CDW structure and resistance anomaly. The magnetoresistance as a function of temperature does not follow the dependence, $\Delta\rho/\rho(0) \sim \omega_c\tau^n$, and reaches a maximum at ~ 30 K. This magnetoresistance is nearly quenched at high electric fields due to CDW motion and at low temperatures the threshold electric fields required for motion are reduced by the magnetic field. Changes in the Fermi-surface gapping or magnetic field-enhanced CDW fluctuations could play a role in reducing the threshold electric fields. A detailed mechanism will have to be worked out and further experiments and analysis will be necessary. However, the high-magnetic-field experiments clearly make it possible to study a range of CDW phenomena at low temperatures which would not be accessible in transport experiments at zero magnetic field.

The authors acknowledge many valuable discussions with Professor Leo Falicov, Professor Vittorio Celli, and Professor John Ruvalds. Dr. P. F. Tua and Dr. R. M. Fleming also contributed useful discussion. Larry Rubin and Bruce Brandt provided technical help at the National Magnet Laboratory, and Estelle Phillips provided valuable help in the crystal-growing program. Work above 80 kG was performed at the Francis Bitter National Magnet Laboratory, supported at the Massachusetts Institute of Technology by the National Science Foundation (NSF). This work was supported by NSF Grant No. DMR-81-06095.

- ¹P. Monceau, N. P. Ong, A. M. Portis, A. Meerschaut, and J. Rouxel, *Phys. Rev. Lett.* **37**, 602 (1976).
- ²R. M. Fleming, D. E. Moncton, and D. B. McWhan, *Phys. Rev. B* **18**, 5560 (1978).
- ³R. M. Fleming, *Phys. Rev. B* **22**, 5606 (1980).
- ⁴J. W. Brill, N. P. Ong, J. C. Eckert, J. W. Savage, S. K. Khana, and R. B. Somoano, *Phys. Rev. B* **23**, 1517 (1981).
- ⁵H. Fröhlich, *Proc. R. Soc. London, Ser. A* **223**, 296 (1954).

- ⁶M. P. Everson, G. Eiserman, A. Johnson, and R. V. Coleman, *Phys. Rev. Lett.* **52**, 1721 (1984).
- ⁷M. P. Everson, G. Eiserman, A. Johnson, and R. V. Coleman, *Phys. Rev. B* **30**, 3582 (1984).
- ⁸John Bardeen, *Phys. Rev. Lett.* **42**, 1498 (1979).
- ⁹N. P. Ong, J. W. Brill, J. C. Eckert, J. W. Savage, S. K. Khana, and R. B. Somoano, *Phys. Rev. Lett.* **42**, 811 (1979).
- ¹⁰John Bardeen, *Phys. Rev. Lett.* **45**, 1978 (1980).